

Satellite measurements of daily variations in soil NO_x emissions

Timothy H. Bertram,¹ Andreas Heckel,³ Andreas Richter,³ John P. Burrows,³
and Ronald C. Cohen^{1,2}

Received 13 September 2005; revised 17 October 2005; accepted 15 November 2005; published 24 December 2005.

[1] Soil NO_x emission from agricultural regions in the western United States has been investigated using satellite observations of NO₂ from the SCIAMACHY instrument. We show that the SCIAMACHY observations over a 2 million hectare agricultural region in Montana capture the short intense NO_x pulses following fertilizer application and subsequent precipitation and we demonstrate that these variations can be reproduced by tuning the mechanistic parameters in an existing model of soil NO_x emissions.

Citation: Bertram, T. H., A. Heckel, A. Richter, J. P. Burrows, and R. C. Cohen (2005), Satellite measurements of daily variations in soil NO_x emissions, *Geophys. Res. Lett.*, 32, L24812, doi:10.1029/2005GL024640.

1. Introduction

[2] Accurate estimates of NO_x (NO_x ≡ NO + NO₂) emissions are critical to our understanding of tropospheric ozone (O₃), biogenic secondary aerosol formation and the biogeochemical cycling of nitrogen. Outside of cities, soil emissions represent a major contribution to the local NO_x budget. Yet characterization of the source strength of soil NO_x (NO_{x,s}) emission on regional and global scales has proven difficult due to the spatial and temporal heterogeneity of the NO_{x,s} flux [Matson *et al.*, 1989]. Reactive nitrogen is predominantly emitted from the soil as nitric oxide (NO), however since NO rapidly reaches steady-state with nitrogen dioxide (NO₂) it is custom to represent NO emissions in terms of NO_x. NO_{x,s} emissions are a complex function of soil moisture and texture, inorganic nitrogen availability, the carbon to nitrogen ratio and canopy structure, coupled to climatic controls such as temperature and precipitation [Firestone *et al.*, 1989]. The variability in NO_{x,s} emission rates are further complicated by soil cultivation and fertilization [Bouwman *et al.*, 2002]. In this study we show that satellite observations of the NO₂ column from SCIAMACHY (SCanning Imaging Absorption spectroMeter for Atmospheric CHartography) capture detailed variations in NO_{x,s} emission on daily time scales with spatial resolution of 30 × 60 km². We use the SCIAMACHY observations to constrain the mechanistic parameters that drive NO_{x,s} emission directly from a 2 million hectare agricultural region in north-central Montana.

¹Department of Chemistry, University of California, Berkeley, California, USA.

²Also at Department of Earth and Planetary Science, University of California, Berkeley, California, USA.

³Institute of Environmental Physics and Remote Sensing, University of Bremen, Bremen, Germany.

[3] Recent attempts to capture the spatio-temporal heterogeneity in NO_{x,s} emission have either extrapolated local scale experiments to the global scale based on simple parameterizations, or used ecosystem process modeling approaches incorporating both climatic and edaphic controls to estimate trace gas emission. Yienger and Levy [1995] (hereinafter referred to as YL), following Williams *et al.* [1992], described a method for extrapolation that calculates a global NO_{x,s} inventory capable of capturing both enhancements in NO_{x,s} emission driven by fertilizer and precipitation, and suppression due to canopy effects. The inventory is based on temperature dependent, biome-specific emission rates driven by climatic fields from a parent general circulation model (GCM), and the Food and Agriculture Organization (FAO) of the United Nations per-country annual fertilizer rates. In contrast, process models, such as the Carnegie-Ames-Stanford (CASA) biosphere model, derive NO_x emission rates directly from estimates of nitrogen mineralization and soil water content based on known soil and litter types, but do not account for fertilizer nitrogen inputs on the global scale [Potter *et al.*, 1996]. Extension of the CASA model to the regional scale has been successful in integrating local climatic fields with regional fertilizer estimates to derive NO_x soil fluxes with spatial resolution better than 10 km [Davidson *et al.*, 1998]. At present, global models such as GEOS-CHEM, MOZART-2 and ECHAM4 employ the YL model (or modifications thereof) as an a priori for global NO_{x,s} emissions [Bey *et al.*, 2001; Hein *et al.*, 2001; Horowitz *et al.*, 2003].

[4] Recent global inverse modeling studies using the Global Ozone Monitoring Experiment (GOME) NO₂ columns with the GEOS-CHEM model, and subsequent partitioning of NO_x source strengths, have revealed nearly a factor of two underestimate in global NO_{x,s} emission with respect to the YL a priori estimate [Jaeglé *et al.*, 2005; Martin *et al.*, 2003]. Agricultural regions such as the western United States show strong disagreement between the a priori estimate and top-down inventory (0.41 vs. 1.0 Tg N year⁻¹) [Jaeglé *et al.*, 2005]. These previous global modeling studies use a priori information on NO_x emissions from fuel combustion and space-based observations of fires to partition the total monthly averaged GOME top-down NO_x emission estimate between fuel combustion, biomass burning and soil emissions in 2° × 2.5° grid boxes.

2. Top-Down NO_x Emission Estimates

[5] Nitrogen dioxide tropospheric column densities were calculated from radiances measured by SCIAMACHY, which flies aboard ENVISAT in a sun synchronous orbit crossing the equator at 10:00 AM local time [Burrows *et al.*, 1995]. With a 960 km swath width and 30 × 60 km² ground

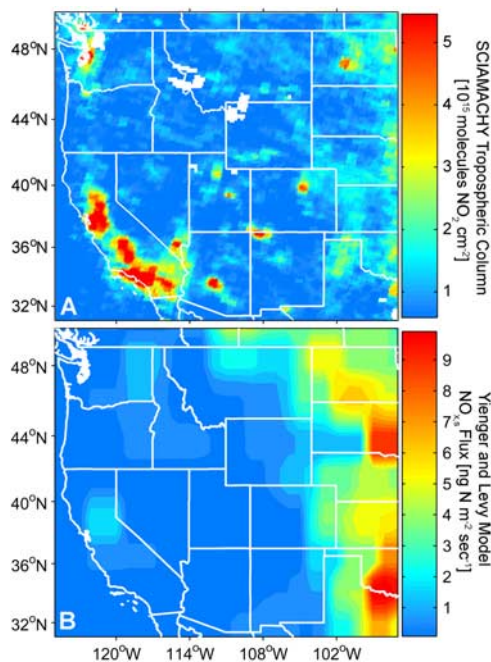


Figure 1. (a) SCIAMACHY derived tropospheric NO₂ vertical column densities over the western United States during May 2004. (b) May NO_{x,s} emission as estimated by Yenger and Levy [1995].

footprint, SCIAMACHY achieves equatorial global coverage in 6 days. Briefly, slant column densities were calculated using Differential Optical Absorption Spectroscopy (DOAS) in the spectral window between 425–450 nm [Richter *et al.*, 2004, 2005]. Cloud filtered slant column densities (using a cloud cover threshold of 30%), corrected for contributions from stratospheric NO₂, were converted to vertical column densities using monthly air mass factors based on vertical NO₂ profiles from the MOZART-2 model [Horowitz *et al.*, 2003].

[6] Top down inventories of NO_x emissions for comparison with existing model inventories were calculated from SCIAMACHY tropospheric NO₂ vertical column densities, the NO_x lifetime (τ_{NO_x}) and the NO₂ to NO_x ratio following the methodology of Martin *et al.* [2003]. NO_x lifetimes, with respect to oxidation by OH, were calculated using diurnally averaged OH fields [Spivakovsky *et al.*, 2000]. The nocturnal sink of NO_x to N₂O₅ (via NO₃) was calculated using local monthly mean temperatures and assuming aerosol scavenging of N₂O₅ occurred with unit efficiency

over the course of a night. The calculated NO_x lifetime and NO₂/NO_x ratio ranged between 10 and 35 hours and 0.6 and 0.8 respectively, for the observation window described in the ensuing section.

[7] The combined error in the calculated NO_x emission rate stems primarily from uncertainty in the factors contributing to the estimated NO_x lifetime coupled to errors in the retrieved NO₂ tropospheric vertical column density [Boersma *et al.*, 2004]. In the region described in this study, we estimate a conservative upper limit to the total uncertainty in the calculated NO_x emissions to be 75%, dominated by the uncertainty in the OH concentration and the small tropospheric excess slant column density. However, due to strong homogeneity in two of the main error sources of the satellite data (aerosol scattering and the NO₂ profile shape) coupled with small cloud fractions in the observation window, the day-day relative uncertainty of the calculated emissions in this region are estimated to be no greater than 35%.

3. Discussion

[8] On the global scale, NO_{x,s} accounts for less than 25% of total NO_x emissions [Jaeglé *et al.*, 2005; Martin *et al.*, 2003]. However, spatial segregation of anthropogenic and biogenic NO_x emissions, coupled to a short boundary layer lifetime of NO_x, results in substantial areas of the world where the local NO_x budget is controlled exclusively by soil emissions. Figure 1a shows monthly averaged NO₂ vertical column densities over the western U.S. as derived from SCIAMACHY measurements during May 2004. Urban centers such as Los Angeles, San Francisco and Denver are evident, as are large point sources such as the Four Corners (36.69°N 108.47°W) and San Juan Generating Station (36.8°N 108.34°W) Utility Plants in San Juan Co., New Mexico. Additionally, large areas of elevated diffuse NO₂ column densities are apparent over much of the Midwest, including most of western Nebraska and Kansas in addition to smaller isolated patches in both North and South Dakota and Northern Montana. These regions are highly correlated with heavily cultivated and fertilized soils. Estimates from the YL NO_{x,s} emission inventory, driven by the temperature and precipitation fields used in the original analysis of YL, are presented in Figure 1b. Application of the YL NO_{x,s} model will differ among various global models depending on the meteorological fields used.

[9] To illustrate the potential of using the SCIAMACHY data for defining the mechanisms responsible for NO_{x,s} emission and to provide constraints for existing models,

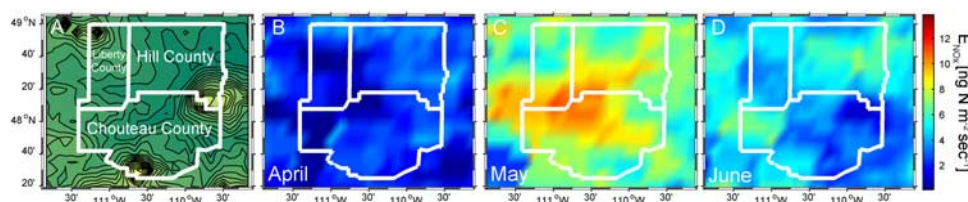


Figure 2. (a) Topographical map of Chouteau, Hill and Liberty Counties in North-Central Montana. The three counties: (i) cover a total of 2.16 million hectares, (ii) contain 0.46 million hectares of harvested cropland, (iii) sustain a population less than 25,000 and (iv) are absent of any major stationary NO_x sources. (b)–(d) April, May and June 2004 monthly averaged NO_x emissions as derived from SCIAMACHY NO₂ columns.

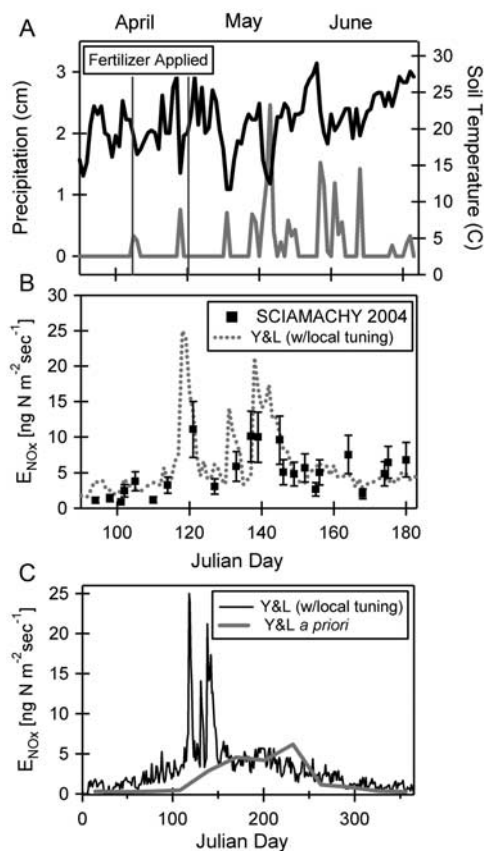


Figure 3. (a) Daily precipitation (gray solid line) and derived soil temperature (black solid line) measured at 10 field sites in Chouteau, Hill and Liberty Counties during April, May and June 2004. Nitrogen fertilizer was applied evenly during the last two weeks of April. (b) Top-down NO_x flux (solid squares) as derived from 2004 SCIAMACHY radiances and the bottom-up NO_{x,s} flux (gray dashed line) as derived from the locally tuned YL model. The error bars in Figure 3b represent the relative error of $\pm 35\%$. (c) Annual profile in NO_{x,s} emissions ($\text{ng N m}^{-2} \text{sec}^{-1}$) as derived from the locally tuned YL model (black solid line) and as described by the YL a priori NO_{x,s} inventory (gray solid line).

we examine in detail one of many agricultural regions apparent in Figure 1a where our calculated top-down NO_x emissions are not likely to be affected by anthropogenic NO_x sources: Chouteau, Hill and Liberty Counties [$47.5\text{--}49^\circ\text{N}$, $109.5\text{--}111.5^\circ\text{W}$] in North-Central Montana (Figure 2a). Spring wheat is the dominant crop grown in this region ($>70\%$ of harvested cropland) [National Agricultural Statistics Service (NASS), 2002], and is primarily fertilized and seeded in mid-April. Nitrogen fertilizer in this region is applied via surface broadcast in the form of urea at $6.7 \pm 2 \text{ g N m}^{-2} \text{ year}^{-1}$ (R. Engel, private communication) and less than 2% of harvested cropland was actively irrigated [NASS, 2002].

[10] Numerous modeling and chamber studies have shown significant enhancements in NO_{x,s} emission following fertilizer application [Akiyama *et al.*, 2003; Bouwman *et al.*, 2002]. For example, Akiyama and Tsuruta observed nearly 100% of the emitted yearly NO flux (0.98% of

applied N) during the cultivation period (42 days) following fertilizer application (broadcast application of urea at 15 g N m^{-2}). Additionally, similar enhancements in NO_{x,s} fluxes have been observed following precipitation events [Davidson, 1992; Jaeglé *et al.*, 2004], where water stressed nitrifying bacteria are activated, resulting in intense pulses of NO_x. The coupling of these two processes presents a significant avenue for enhanced NO_{x,s} emission from agriculture directly following fertilizer application [Hall *et al.*, 1996]. The spatial and temporal heterogeneity resulting from these processes can be seen in the SCIAMACHY derived NO_x emission rates over the Montana farmlands during April, May and June of 2004 (Figures 2b–2d). The enhancement in NO_x emission during May 2004 is a direct result of heavy fertilization of dry cropland in late April coupled to strong rains in early May (Figure 3a). Similar enhancements to those shown in Figure 2 were also observed in May 2003. No other NO_x source is consistent with the observations. During April–June 2004 no significant fires were observed over north-central Montana that correspond with the NO₂ enhancements observed from SCIAMACHY [National Environmental Satellite, Data, and Information Service (NESDIS), 2004a].

[11] Currently, global NO_{x,s} emissions based on the YL model use country averaged FAO N-fertilizer inputs, distribute the fertilizer evenly in time during the growing season, constrain the yearly flux to a fixed percentage of applied nitrogen (2.5%) and use either GCM or assimilated meteorological fields. This approach prevents current empirical models from capturing the temporal heterogeneity that we observe in the space-based imaging and limits their utility for identifying and evaluating the model representation of the underlying processes responsible for NO_{x,s} emission.

[12] Figure 3a illustrates the mean precipitation and calculated soil temperatures from 10 field stations in the observation area [NESDIS, 2004b; Williams *et al.*, 1992]. Figure 3b depicts the daily SCIAMACHY derived NO_x emissions for the three county observation area. The strongest NO_x emissions occur following crop fertilization and are enhanced by subsequent precipitation events. Using local climatology and fertilizer application practices the YL model can be used to reproduce the emissions as observed from SCIAMACHY (Figure 3b). In our analysis: (i) we used the measured local temperature and precipitation fields [NESDIS, 2004b], (ii) we applied fertilizer at $6.7 \pm 2 \text{ g N m}^{-2} \text{ year}^{-1}$ evenly during the last two weeks of April, allowing the available fertilizer to decay to zero by the end of the growing season to emulate plant uptake of available nitrogen and washout by rains and (iii) we constrained the fraction of applied nitrogen emitted as NO_x to 0.7% [Bouwman *et al.*, 2002]. Finally, we tune the YL empirical precipitation enhancement factors to capture the structure and magnitude observed in the SCIAMACHY NO₂ columns. Specifically, we redefined the requirements for soil water saturation (soil was considered saturated if the 10-day precipitation total exceeded 2 cm as opposed to the a priori of 1 cm over 14 days) and the requisite rain thresholds were increased from 0.1, 0.5, 1.5 cm day⁻¹ to 0.5, 0.75, 1.5 cm day⁻¹ for the varying degrees of precipitation enhancement to reproduce the detailed structure in the observed emissions.

[13] The 2004 annual profiles in NO_{x,s} emission for Chouteau, Hill and Liberty counties, as calculated using the locally tuned YL model and as described by the YL NO_{x,s} a priori, are shown in Figure 3c. The locally tuned YL model reproduces the enhancement in NO_x emission observed by SCIAMACHY following fertilizer application, underlining the importance of a proper representation of the timing of N-fertilizer application and precipitation pulsing.

4. Concluding Remarks

[14] This analysis of satellite observations of NO₂ enhancements over agricultural regions during and directly following fertilization provides new insight on the spatial and temporal heterogeneity in NO_{x,s} emission on the regional scale. For the agricultural region in North-Central Montana, described in this study, we calculate a yearly SCIAMACHY top-down estimate 60% higher than the YL a priori estimate, consistent with the discrepancies observed by Jaeglé *et al.* [2005] over the western United States using monthly averaged GOME data. The quality of the SCIAMACHY data is such that future inverse modeling studies, constructed to partition NO_x source emissions, could extend beyond the Jaeglé *et al.* analysis by tuning the mechanistic parameters which drive NO_{x,s} emissions in the inversion of the satellite observation. This approach would aid in resolving the short intense pulses observed by SCIAMACHY that current a priori estimates are unable to capture and it should allow for a direct constraint on soil moisture from space-based measurements. Further, it would allow for assessment of the variability in the YL parameters across the globe, essential for proper representation of these parameters in current global models. Future comparison of satellite derived NO_{x,s} emission with locally tuned empirical models (e.g., YL) and with more sophisticated process based models (e.g. CASA) on the regional scale would be instructive in determining accurate NO_{x,s} emission estimates necessary to address current questions in atmospheric chemistry.

[15] **Acknowledgments.** SCIAMACHY lv0 and lv1 spectra were provided by ESA through DFD/DLR. We thank Richard E. Engel of the Department of Land Resources and Environmental Services at Montana State University for helpful discussions regarding fertilizer application practices in Montana. This work was supported in part through the University of Bremen, NOAA and by NASA grant NAGS-13688.

References

- Akiyama, H., *et al.* (2003), Nitrous oxide, nitric oxide, and nitrogen dioxide fluxes from soils after manure and urea application, *J. Environ. Qual.*, *32*, 423–431.
- Bey, I., *et al.* (2001), Global modeling of tropospheric ozone: Implications for dynamics and biomass burning, *J. Geophys. Res.*, *106*, 23,073–23,095.
- Boersma, K. F., H. J. Eskes, and E. J. Brinkman (2004), Error analysis for tropospheric NO₂ retrieval from space, *J. Geophys. Res.*, *109*, D04311, doi:10.1029/2003JD003962.
- Bouwman, A. F., L. J. M. Boumans, and N. H. Batjes (2002), Modeling global annual N₂O and NO emissions from fertilized fields, *Global Biogeochem. Cycles*, *16*(4), 1, 1080, doi:10.1029/2001GB001812.
- Burrows, J. P., *et al.* (1995), SCIAMACHY—Scanning Imaging Absorption Spectrometer for Atmospheric Cartography, *Acta Astronaut.*, *35*, 445–451.
- Davidson, E. A. (1992), Pulses of nitric oxide and nitrous oxide flux following wetting of dry soil: An assessment of probable sources and importance relative to annual fluxes, *Ecol. Bull.*, *42*, 149–155.
- Davidson, E. A., *et al.* (1998), Model estimates of regional nitric oxide emissions from soils of the southeastern United States, *Ecol. Appl.*, *8*, 748–759.
- Firestone, M. K., *et al.* (1989), Microbial basis of NO and N₂O production and consumption in soil, in *Exchange of Trace Gases Between Terrestrial Ecosystems and the Atmosphere*, pp. 7–21, John Wiley, Hoboken, N. J.
- Hall, S. J. (1996), NO_x emissions from soil: Implications for air quality modeling in agricultural regions, *Annu. Rev. Energy Environ.*, *21*, 311–346.
- Hein, R., *et al.* (2001), Results of an interactively coupled atmospheric chemistry–general circulation model: Comparison with observations, *Ann. Geophys.*, *19*, 435–457.
- Horowitz, L. W. (2003), A global simulation of tropospheric ozone and related tracers: Description and evaluation of MOZART, version 2, *J. Geophys. Res.*, *108*(D24), 4784, doi:10.1029/2002JD002853.
- Jaeglé, L., R. V. Martin, K. Chance, L. Steinberger, T. P. Kurosu, D. J. Jacob, A. I. Modi, V. Yoboué, L. Sigha-Nkamdjou, and C. Galy-Lacaux (2004), Satellite mapping of rain-induced nitric oxide emissions from soils, *J. Geophys. Res.*, *109*, D21310, doi:10.1029/2004JD004787.
- Jaeglé, L., *et al.* (2005), Global partitioning of NO_x sources using satellite observations: Relative roles of fossil fuel combustion, biomass burning and soil emissions, *Faraday Discuss.*, *130*, 1–17.
- Martin, R. V., D. J. Jacob, K. Chance, T. P. Kurosu, P. I. Palmer, and M. J. Evans (2003), Global inventory of nitrogen oxide emissions constrained by space-based observations of NO₂ columns, *J. Geophys. Res.*, *108*(D17), 4537, doi:10.1029/2003JD003453.
- Matson, P. A., *et al.* (1989), Regional extrapolation of trace gas flux based on soils and ecosystems, in *Exchange of Trace Gases Between Ecosystems and the Atmosphere*, pp. 97–108, John Wiley, Hoboken, N. J.
- National Agricultural Statistics Service (2002), 2002 Census of Agriculture, <http://www.nass.usda.gov/census/>, U. S. Dep. of Agric., Washington, D. C.
- National Environmental Satellite, Data, and Information Service (NESDIS) (2004a), Hazard Mapping System Fire and Smoke Product, <http://www.ssd.noaa.gov/PS/FIRE/hms.html>, Natl. Oceanic and Atmos. Admin., Silver Spring, Md.
- National Environmental Satellite, Data, and Information Service (NESDIS) (2004b), National Climatological Data, <http://nmdc.noaa.gov>, *Natl. Clim. Data Cent.*, Natl. Oceanic and Atmos. Admin., Silver Spring, Md.
- Potter, C. S., *et al.* (1996), Process modeling of controls on nitrogen trace gas emissions from soils worldwide, *J. Geophys. Res.*, *101*, 1361–1377.
- Richter, A., V. Eyring, J. P. Burrows, H. Bovensmann, A. Lauer, B. Sierk, and P. J. Crutzen (2004), Satellite measurements of NO₂ from international shipping emissions, *Geophys. Res. Lett.*, *31*, L23110, doi:10.1029/2004GL020822.
- Richter, A., *et al.* (2005), Increase in tropospheric nitrogen dioxide over China observed from space, *Nature*, *437*, 129–132.
- Spivakovsky, C. M., *et al.* (2000), Three-dimensional climatological distribution of tropospheric OH: Update and evaluation, *J. Geophys. Res.*, *105*, 8931–8980.
- Williams, E. J., *et al.* (1992), An inventory of nitric oxide emissions from soils in the United States, *J. Geophys. Res.*, *97*, 7511–7519.
- Yienger, J. J., and H. Levy (1995), Empirical model of global soil-biogenic NO_x emissions, *J. Geophys. Res.*, *100*, 11,447–11,464.

T. H. Bertram and R. C. Cohen, Department of Chemistry, University of California, Berkeley, Berkeley, CA 94720–1640, USA. (cohen@cchem.berkeley.edu)

J. P. Burrows, A. Heckel, and A. Richter, Institute of Environmental Physics and Remote Sensing, University of Bremen, D-28344 Bremen, Germany.